Kinetic theory of polymer crystal growth applied to melt crystallization of low molecular weight poly(ethylene oxide)*

C. P. Buckley
Department of Textile Technology, UMIST, Manchester M60 1QD, UK
(Received 5 June 1979; revised 24 September 1979)

The kinetic theory of polymer crystal growth from the melt is extended to polymers with finite molecular weight and small numbers of folds per molecule. The theory is applied specifically to poly(ethylene oxide), where the most detailed experimental data are available on the growth of crystals from low molecular weight fractions. Predicted curves of growth-rate *versus* temperature show extensive qualitative agreement with experiment, including increasing chain-folding with increasing molecular weight or supercooling. In the theory this arises from the assumption that molecules have no freedom of lengthwise position within a surface nucleus. It may provide a general rationalization for chain-folding, but could possibly be a consequence of end-group pairing in the special case of OH-terminated poly(ethylene oxide). The theory also explains the sharpness of observed transitions between growth-modes with different numbers of folds per molecule, and the changes in shape of crystals near the transition. Reasonable quantitative agreement with experiment is found in the two cases of high molecular weight and high degrees of supercooling. For low molecular weights and small supercoolings, however, there is a large quantitative discrepancy between the predicted and observed separations of adjacent branches of each growth-rate/temperature curve. This appears to be inexplicable in terms of existing understanding of polymer crystal growth. An Appendix is given which outlines the effects on the theory of relaxing various assumptions of the growth model.

INTRODUCTION

Perhaps the most remarkable property of long-chain molecules is their tendency to crystallize in folded conformation. This behaviour is now well-documented for a wide range of polymers, but its cause remains unclear. It is, however, widely believed to be kinetic in origin. A direct means of tackling the problem is to study the crystallization rate of low molecular weight (*MW*) polymers, in the régimes of *MW* and supercooling where the transition from extended-chain to folded-chain crystal growth can be observed. If the results of experiments such as this could be interpreted properly, the problem of explaining chain-folding would be solved.

Detailed data of this type have now been obtained for melt-crystallization of low *MW* fractions of polyethylene (PE)[1,2] and poly(ethylene oxide) (PEO)[3–6]. The remaining problem is that of interpretation of the data. Current understanding of polymer melt crystallization rests on a kinetic theory which assumes *MW* to be infinite, and which is therefore inapplicable in its present form. It is not sufficient merely to substitute the appropriate (*MW*-dependent) equilibrium melting-point into the existing theory[1]. The occurrence of chain-ends changes the sequence of molecular events involved in crystal growth, and makes a more drastic revision of the theory necessary. Previous kinetic theories allowing for finite *MW* have used the approximate 'saddle-point' approach[7,8]. A detailed theory was, however, developed by Sanchez and DiMarzio[9] for crystallization from dilute solution. Some of their findings are relevant to the present case.

To construct a theory of the growth process, one must answer rather detailed questions on the structure of low *MW* polymer crystals. Are chain-ends always rejected or are some incorporated as defects within the crystal? Is there the same number of folds per molecule? How long are the cilia protruding from the crystal surface? Of course, these questions do not arise if the *MW* can be assumed infinite. In the case of PE, results so far are ambiguous on these points[1,2]. PEO, on the other hand, crystallizes in an unusually well-defined manner for a polymer system, and these details are known with sufficient certainty to allow progress in modelling the crystallization process.

Our purpose in the present work has been to exploit the PEO system for testing current understanding of polymer crystallization from the melt. In particular, can it account for the transition from extended to folded-chain crystal growth with increasing supercooling or *MW*?

We take as a starting point the model of polymer crystal growth originally proposed by Lauritzen and Hoffman[10], which has found wide application to high *MW* polymers with high degrees of chain-folding. Later modifications due to Lauritzen and Hoffman[11] and Lauritzen[12] are included, but are of only minor importance here. Changes are introduced as necessary for application to polymers of finite *MW*, where the number of folds per molecule may be small or even zero. Where detail is required the specific case of low *MW* PEO is invoked. Even then, several points of ambiguity remain; and it has proved necessary to formulate various versions of the theory, embodying different assumptions. The version given in detail below is the

* A shortened version of this paper was presented at the Biennial Conference of the Institute of Physics Polymer Physics Group, held at Shrivenham, UK, September 1977

0032–3861/80/040436–14$02.00

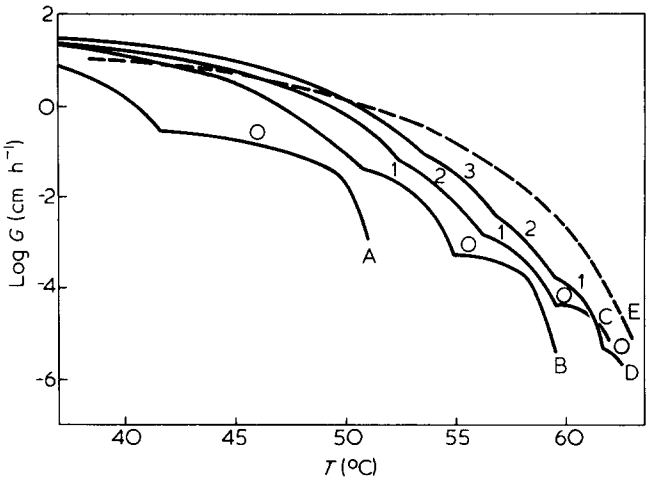

Figure 1 Crystal growth-rate G *versus* temperature T for four low *MW* fractions of PEO: A, M_n = 1890; B, M_n = 3900; C, M_n = 5970; D, M_n = 7760 and one high *MW* sample: E, M_η = 152 000 after Kovacs and coworkers[3–5]. Parameter shown is n, the number of folds per molecule

most straightforward extension of the existing theory. More complex modifications are outlined in the Appendix. They were found to offer no practical advantage in fitting experimental data.

Crystal growth-rates predicted by the theory have been computed using thermodynamic parameters for PEO. They are compared with published growth-rate data for this system.

THEORY

The case of low MW PEO

Bulk samples of low *MW* fractions of hydroxyterminated PEO, crystallized from the melt, have been shown to have crystal thicknesses L corresponding to integral fractions of the molecular length λ (i.e. $L \simeq \lambda/(n+1)$ where n is an integer)[13–15]. This indicates that each molecule is folded exactly a small number of times, n, with chain-ends residing in the crystal surface and chain-folds being rather 'tight' with adjacent re-entry. Thermodynamic measurements, which allowed estimates to be made of the lengths of chain-folds and cilia[16], confirmed this. The crystals thicken in a stepwise manner to $n-1$ folds per molecule with increasing crystallization time or temperature, and during subsequent annealing[3,17]. The rate of unfolding is a strong function of L, decreasing with increasing L[16], consistent with it being limited by the rate of dragging a hydroxyl end-group through the crystal. All of this behaviour shows that it is much less energetically favourable for PEO chain-ends to lie inside, rather than outside, the crystal. On these grounds we shall assume that incorporation of chain-ends within the crystal during growth can be neglected.

Graphs of measured crystal growth-rate G *versus* temperature T for melt-grown single crystals or spherulites show distinct branches[3], corresponding to each integral value of n (see *Figure 1*). Each branch has the qualitative shape of the $G(T)$ curve for a typical high *MW* polymer, including giving approximately the characteristic linear relation between $\log G$ and $1/T\Delta T$, where ΔT is the appropriate (*MW*-dependent) supercooling[3]. Yet, in the high *MW* case, this shape, according to the theory of Lauritzen and Hoffman[10], results from the *continuous* variation of L (or strictly of surface nucleus thickness) with T, contradicting the apparent situation in low *MW* PEO.

We resolve the paradox as follows. We assume that crystal growth in this system does occur by coherent surface nucleation involving nuclei with, say, n folds per molecule and a thickness l which varies with T, as in the high *MW* case. But we further assume that a nucleus rapidly thickens after formation, as much as possible without any unfolding and hence without dragging chain-ends into the crystal. If the lengthwise positioning of molecules in the nucleus is correct (as might be the case if some hydrogen-bond hydroxyl-group pairing exists between molecules in the crystal and those nearby in the melt) this could be accomplished with little or no longitudinal diffusion. The final thickness will therefore be approximately $\lambda/(n+1)$ and will correspond to the thickness L measured on mature crystals. This thickening can be shown to occur in a time less than that required for nucleation. A new nucleus therefore always 'sees' a substrate of thickness L.

Further assumptions employed here are that all molecules have the same length λ and are deposited with the same number of folds, n, within a given branch of the $G(T)$ curve.

Model of growth process

The polymer crystal is taken to be lamellar in shape, with molecular axes normal to its large surfaces. In common with most previous treatments of polymer crystal growth, we assume the crystal to grow by coherent secondary nucleation of a new surface patch onto the growth face, followed by one-dimensional lateral growth of the patch along the face to complete a new monomolecular layer. A new feature, however, is that a crystal growing with given n and λ is assumed to always present a growth face of thickness $L \simeq \lambda/(n+1)$, for reasons given above.

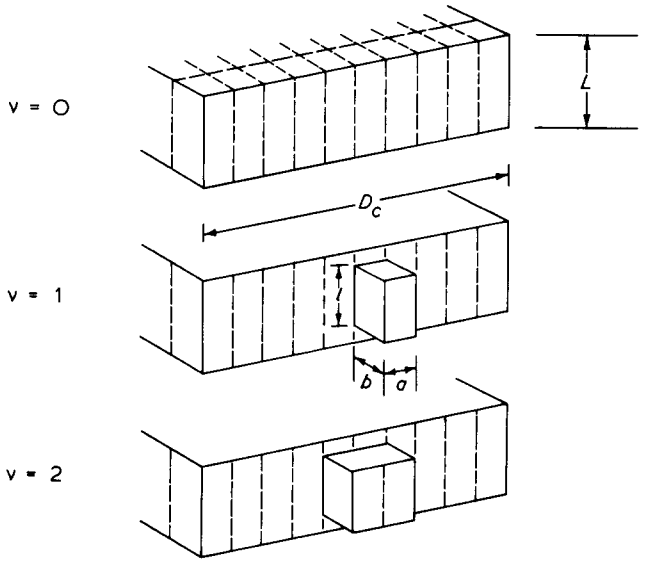

Figure 2 First few stages in the formation of a surface nucleus on a crystal growth-face

The growth process is illustrated in *Figure 2* as a sequence of many stages, the vth stage corresponding to the patch containing some whole number v of molecular stems arranged side-by-side. Each stem is represented by a box of depth b, width a and height l. We assume that l does not fluctuate within a growth layer, but it may between layers. The crystal substrate is shown to have a finite width D_c, following Lauritzen[12]. This corresponds to the distance between crystal defects over which crystallographic regularity is maintained. We assume $D_c \gg a$.

The above is clearly a coarse model of the process. In reality, the deposition of each stem presumably consists of the sequential deposition of individual main-chain atoms. We prefer the coarse approach here to make the analysis less cumbersome. Its justification has been considered by previous authors[9,18]*.

The growth process can therefore be considered as a 'sequential process', discussed in this context by Frank and Tosi[18]. Moreover, with the assumptions introduced above, we can concentrate on the case where there is only one possible sequence of stages, which is the case treated by Frank and Tosi. DiMarzio[19] has given a more general formulation which would be necessary, for example, if fluctuations of λ, n or l were to be included.

We thus consider an ensemble in which η_v is the occupation number of the vth stage and α_v, β_v are the forward and backward transition rates from this stage. Assuming steady-state conditions, with no 'piling-up' in any of the stages, the net forward flux j was shown to be given by[18]:

$$j = \frac{\alpha_v \eta_v}{\left[1 + \sum_{m=v+1}^{\infty} \prod_{i=v+1}^{m} \gamma_i\right]} \tag{1}$$

where $\gamma_i = \beta_i/\alpha_i$.

Lauritzen[12] has pointed out that growth of a polymer crystal can be of one of two types. He labels *Régime 1* the situation where growth is limited by the rate of secondary nucleation. A surface patch once nucleated spreads to cover the substrate in a time much less than the nucleation time, leaving a smooth substrate for the next nucleus. The other possibility is *Régime 2*, where the time taken to complete a new growth layer is greater than the nucleation time. This results in multiple nucleation, leaving the crystal with a rough edge. We consider each possibility in turn.

Régime 1

In the above notation, new nuclei of thickness l form at a rate $j(l)$ for η_0 available sites. On the substrate in *Figure 2* we can assume that there are D_c/a such sites and hence the total nucleation rate J per growth face is given by:

$$J = \frac{D_c}{a} \Sigma [j(l)/\eta_0] \tag{2}$$

where the summation is over all possible values of l (see below) and j/η_0 is given from equation (1) as:

* The author has found by detailed calculation that the present theory leads to essentially the same results when formulated using the fine-grained approach, considering the attachment of successive main-chain atoms

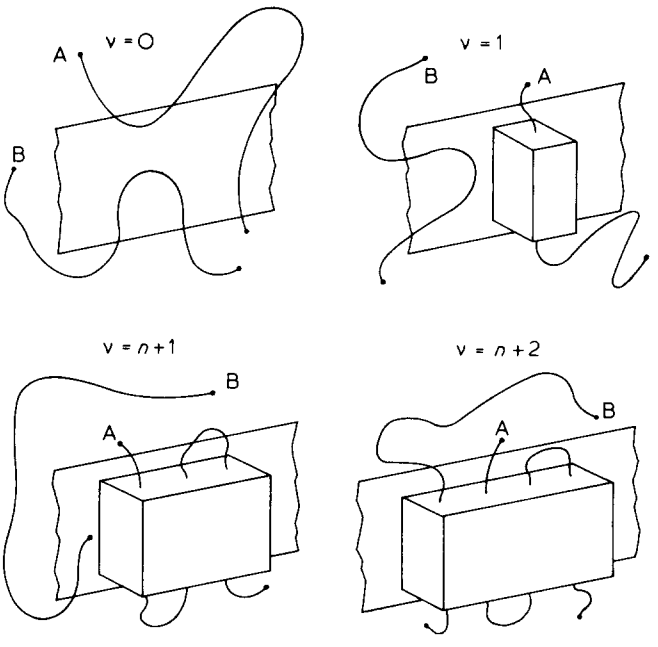

Figure 3 Schematic diagram of molecular events assumed in the formation of a surface nucleus

$$\frac{j}{\eta_0} = \frac{\alpha_0}{\left[1 + \sum_{m=1}^{\infty} \prod_{i=1}^{m} \gamma_i\right]} \tag{3}$$

To evaluate j/η_0, it is necessary to define the sequence more precisely. We shall assume here that the sequence of adding new stems follows the pattern shown in *Figure 3*. The molecules are laid down sequentially, each one being folded n times before deposition of the next. If all molecules lie down in an identical manner the surface patch must be periodic in v, with:

$$\gamma_v = \gamma_{v+n+1} \qquad (v > 0) \tag{4}$$

In this case equation (3) may be expressed in closed form:

$$\frac{j}{\eta_0} = \frac{\alpha_0\left[1 - \prod_{i=1}^{n+1} \gamma_i\right]}{\left[1 + \sum_{m=1}^{n} \prod_{i=1}^{m} \gamma_i\right]} \tag{5}$$

Here we shall make the further simplification that there are only three distinct α_v:

$$\alpha_0; \quad \alpha_1 = \alpha_2 = \ldots \alpha_n = \alpha; \quad \alpha_{n+1} = \alpha' \tag{6}$$

and one distinct β_v:

$$\beta_1 = \beta_2 = \ldots \beta_{n+1} = \beta \tag{7}$$

(β_0 has no meaning). Equation (5) then becomes:

$$\frac{j}{\eta_0} = \frac{\alpha_0[1 - \gamma^n\gamma']}{\left[1 + \sum_{m=1}^{n} \gamma^m\right]} \tag{8}$$

where $\gamma = \beta/\alpha$, $\gamma' = \beta/\alpha'$.

To evaluate the transition rates it is necessary to construct their corresponding free enthalpy barriers. Let $\Delta\phi_{v,v+1}$ be the barrier for transition from stage v to stage $v+1$. Referring to *Figure 3*, it is clear that the only distinct $\Delta\phi$ arising may be assumed to be (leaving aside the additional barrier height for molecular diffusion):

$$\left.\begin{aligned}\Delta\phi_{0,1} &= 2bl\sigma + 2ab\sigma'_{e0} - \psi abl\Delta f \\ \Delta\phi_{1,0} &= (1-\psi)abl\Delta f \\ \Delta\phi_{1,2} &= 2ab\sigma_{ef} - \psi abl\Delta f \\ \Delta\phi_{n+1,n+2} &= 2ab\sigma'_{e0} - \psi abl\Delta f\end{aligned}\right\} \tag{9}$$

In equations (9), σ is the lateral surface free energy of the crystal and Δf the bulk free enthalpy of fusion per unit volume of crystal. The parameter ψ apportions the bulk free enthalpy change between forward and backward steps and can take values between 0 and 1. It was introduced by Lauritzen and Hoffman[11] to surmount a difficulty which arises at high supercoolings if it is allowed only to be unity. The surface free energies σ_{ef} and σ_{e0} refer to chain-folds and chain-ends respectively. In equations (9), however, we have used $2\sigma'_{e0}$ to denote the combination:

$$2\sigma'_{e0} = 2\sigma_{e0} + \frac{kT}{ab}\ln Cp \tag{10}$$

where k is Boltzmann's constant, C is a constant characteristic of the flexibility of the molecule and p the degree of polymerization. The second term of equation (10), while not a surface energy, occurs in conjunction with σ_{e0}. It corresponds to the entropic free enthalpy gained when a molecule is brought from the melt to a specific point in space, as introduced by Flory and Vrij[20] for analysing the melting of n-paraffins (see also the 'entropy of localization' of Sanchez and DiMarzio[9]). It was found necessary in the analysis of melting of low *MW* PEO by Buckley and Kovacs[21]. Its inclusion here presupposes that each molecule has no choice of lengthwise position within the nucleus, consistent with assuming that crystal thickening from l to L can be achieved without longitudinal diffusion.

The transition rates can now be constructed as follows:

$$\left.\begin{aligned}\alpha_0 &= \mu\exp\left[-\frac{2bl\sigma}{kT} - \frac{2ab\sigma'_{e0}}{kT} + \frac{\psi abl\Delta f}{kT}\right] \\ \alpha &= \mu\exp\left[-\frac{2ab\sigma_{ef}}{kT} + \frac{\psi abl\Delta f}{kT}\right] \\ \alpha' &= \mu\exp\left[-\frac{2ab\sigma'_{e0}}{kT} + \frac{\psi abl\Delta f}{kT}\right] \\ \beta &= \mu\exp\left[-(1-\psi)\frac{abl\Delta f}{kT}\right]\end{aligned}\right\} \tag{11}$$

where μ is the transport term, which for the small supercoolings of interest here can be assumed to have the form $(kT/h)\exp(-E/kT)$, where h is Planck's constant and E an effective activation energy for molecular transport in the melt (assumed independent of *MW*). Substituting from equations (11) into equation (8) then yields:

$$\frac{j}{\eta_0} = \mu\left\{1-\exp\left[\frac{2ab(n\sigma_{ef}+\sigma'_{e0})}{kT} - \frac{(n+1)abl\Delta f}{kT}\right]\right\}\times\left\{1+\sum_{m=1}^{n}\exp\left[\frac{2mab\sigma_{ef}}{kT} - \frac{mabl\Delta f}{kT}\right]\right\}^{-1}$$
$$\times\exp\left[-\frac{2bl\sigma}{kT} - \frac{2ab\sigma'_{e0}}{kT} + \frac{\psi abl\Delta f}{kT}\right] \tag{12}$$

Equation (12) gives the nucleation rate for a particular nucleus thickness l. The form of the function is sketched in *Figure 4*. The lower limit on nucleus thickness, l_{min}, at or below which nuclei do not form is given from equation (12) by:

$$l_{min} = \frac{2(n\sigma_{ef}+\sigma'_{e0})}{(n+1)\Delta f} \tag{13}$$

The upper limit for given λ and n is clearly $L = (\lambda - 2l_{c0} - nl_{f0})/(n+1)$, where l_{c0} and l_{f0} are the lengths of cilia and chain-folds in mature crystals. Otherwise, chain-ends or chain-folds would have to enter the crystal. This is a major departure from the infinite *MW* approximation, which allows l instead to extend to infinity. The cut-off at $l = L$ is the means by which J is

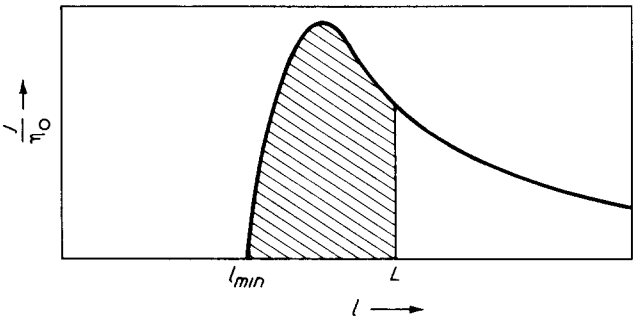

Figure 4 Sketch of the function $j(l)/\eta_0$ given by equation (12)

brought to zero at the melting-point $T_m(\lambda, n)$, since at this temperature $L = l_{min}$. The relevant nucleation rates thus occur only within the shaded part of *Figure 4*.

The crystal growth face advances a distance b in a time J^{-1}. The growth-rate in this regime, G_1, is therefore given from equation (2) by:

$$G_1 = \frac{bD_c}{a} \Sigma [j(l)/\eta_0] \tag{14}$$

where j/η_0 is given by equation (12) and the summation is understood to extend from $l = l_{min}$ to $l = L$, in steps of l_u, the c-axis projection of one main-chain bond.

Régime 2

Let I represent the total nucleation rate per unit length of substrate i.e. $I = J/D_c$; and g the velocity with which a surface patch spreads laterally along the growth face. In régime 2, where g is small and multiple nucleation occurs, the appropriate growth-rate becomes[22]:

$$G_2 = b(Ig)^{1/2} \tag{15}$$

Since, in the present model, a range of values of l are represented on each growth-face, it is necessary to use in equation (15) the mean value of g:

$$\langle g \rangle = \sum \left[g(l) \frac{j(l)}{\eta_0} \right] \Big/ \sum \left[\frac{j(l)}{\eta_0} \right] \tag{16}$$

giving:

$$G_2 = b(I\langle g \rangle)^{1/2} = b \left\{ \sum \left[\frac{g(l)}{a} \frac{j(l)}{\eta_0} \right] \right\}^{1/2} \tag{17}$$

where summations are again from $l = l_{min}$ to $l = L$.

The velocity g will not in general be constant as the patch grows. Its average value for the addition of the υ_0th to the $(\upsilon_0 + n)$th stems is simply the width $a(n + 1)$ of these stems divided by the time taken to add them:

$$g = a(n+1) \Big/ \sum_{\upsilon=\upsilon_0}^{\upsilon_0+n} \left(\frac{\eta_\upsilon}{j} \right) \tag{18}$$

Using equation (1) to provide (η_υ/j), and invoking as before the periodicity of γ_υ (see equation (4)), we may express the summation in equation (18) in closed form:

$$\sum_{\upsilon=\upsilon_0}^{\upsilon_0+n} \left(\frac{\eta_\upsilon}{j} \right) = \frac{\displaystyle\sum_{\upsilon=\upsilon_0}^{\upsilon_0+n} \alpha_\upsilon^{-1} \left[1 + \sum_{m=\upsilon+1}^{\upsilon+n} \prod_{i=\upsilon+1}^{m} \gamma_i \right]}{\left[1 - \displaystyle\prod_{i=\upsilon_0+1}^{\upsilon_0+n+1} \gamma_i \right]} \tag{19}$$

Given the periodicity of α_v and γ_v this expression is independent of v_0 and represents the time taken to add any adjacent sequence of $n+1$ stems (excepting $v_0 = 0$). Under these conditions, therefore, the surface patch does spread with a mean velocity g independent of its size. When the additional simplification of equations (6) and (7) is invoked, equation (19) reduces after manipulation to:

$$\sum_{v=v_0}^{v_0+n} \left(\frac{\eta_v}{j}\right) = \frac{\sum_{m=0}^{n} \gamma^m [\alpha'(n-m)/\alpha + m + 1]}{\alpha'[1-\gamma^n\gamma']} \tag{20}$$

for all $v_0 > 0$. Substituting from equations (11) and (20) into (18) we obtain:

$$g = \mu a(n+1)\left\{1 - \exp\left[\frac{2ab(n\sigma_{ef} + \sigma'_{e0})}{kT} - \frac{(n+1)abl\Delta f}{kT}\right]\right\}$$
$$\times \left[\sum_{m=0}^{n}\left\{1 + m + (n-m)\exp\left[\frac{2ab(\sigma_{ef} - \sigma'_{e0})}{kT}\right]\right\}\exp\left[\frac{2mab\sigma_{ef}}{kT} - \frac{mabl\Delta f}{kT}\right]\right]^{-1}$$
$$\times \exp\left[-\frac{2ab\sigma'_{e0}}{kT} + \frac{\psi abl\Delta f}{kT}\right] \tag{21}$$

The growth-rate G_2 is then given by equation (17), using equation (21) for $g(l)$ and equation (12) for $j(l)/\eta_0$.

We must now consider which regime to expect in a given experiment, a question discussed in detail by Lauritzen[12]. An approximate argument would be as follows. Let τ_n be the average time between nucleation events on a given growth-face and τ_c the time required for completion of a new growth-layer. Clearly, in régime 1 $\tau_n > \tau_c$, and in régime 2 $\tau_n < \tau_c$. To a first approximation $\tau_c^{-1} = g/D_c$ and hence, through equation (21), depends on l. Taking therefore the mean τ_c^{-1} to be $\langle\tau_c^{-1}\rangle = \langle g\rangle/D_c$, and noting $\tau_n^{-1} = J = ID_c$, we may define D_c^* as the value of D_c satisfying $\langle\tau_c^{-1}\rangle = \tau_n^{-1}$, giving:

$$D_c^* = \{\langle g\rangle/I\}^{1/2} \tag{22}$$

Régime 1 prevails when $D_c \ll D_c^*$ and régime 2 when $D_c \gg D_c^*$. To within a constant factor of order unity, equation (22) agrees with the more carefully derived result of Lauritzen[12]. The growth-rate presumably varies smoothly between G_1 and G_2 when D_c is of the same order as D_c^*, but no exact solution of this difficult case is yet available. It proved useful in the present work to use $I = G_1/bD_c$ and $\langle g\rangle = G_2^2/b^2I$ to express equation (22) in the form:

$$D_c^* = G_2/(G_1/D_c) \tag{23}$$

Further comments on theory

The analysis given above introduced several extra assumptions, not yet discussed, which are difficult to justify *a priori*. The following modifications to the theory were therefore examined, to study the effects of systematically relaxing these assumptions. Details are given in the Appendix.

(a) *Choice of sequence* For given λ, n and l a single sequence was assumed, corresponding to each molecule being fully n times folded before addition of the next (see *Figure 5a*). Since, however, the surface patch can grow at either end, a different sequence could occur, such as in *Figure 5b*, without violating the assumption that all molecules fold n times. In the example shown at $v = 3$, a new molecule has arrived before completion of deposition of the first. There are clearly many different sequences that could be followed, and the resulting nucleation rate can in general only be bounded. The expressions for G_1 and G_2 derived above turn out to be the upper limits. The lower limits, corresponding to the sequence in *Figure 5c*, were also calculated and were found to be smaller by a factor of 10 to 100 (excepting $n = 0$, when the two bounds coincide). It also follows that any sequence involving non-adjacent re-entry will lead to growth-rates G_1 and G_2 below those derived from *Figure 5a*. The model therefore predicts that chain-folding, when it occurs, will be by adjacent re-entry.

(b) *Number of nucleation sites* In equation (2) it was assumed that a width a of the substrate contributes only one potential nucleation site. In the present model (*Figure 2*), however, when $L > l$ the nucleus may have a choice of lengthwise position, and a width a will then contribute a number of sites which depends on l.

(c) *Degree of molecular localization* In equation (10) each molecule is assumed to have no freedom in its lengthwise placement in the surface patch. This is necessary if thickening from l to L is to occur without longitudinal diffusion. If this diffusion is allowed to occur, the assumption can be relaxed without making the theory intractible according to one of two models (*Model 1* and *Model 2* – see the Appendix).

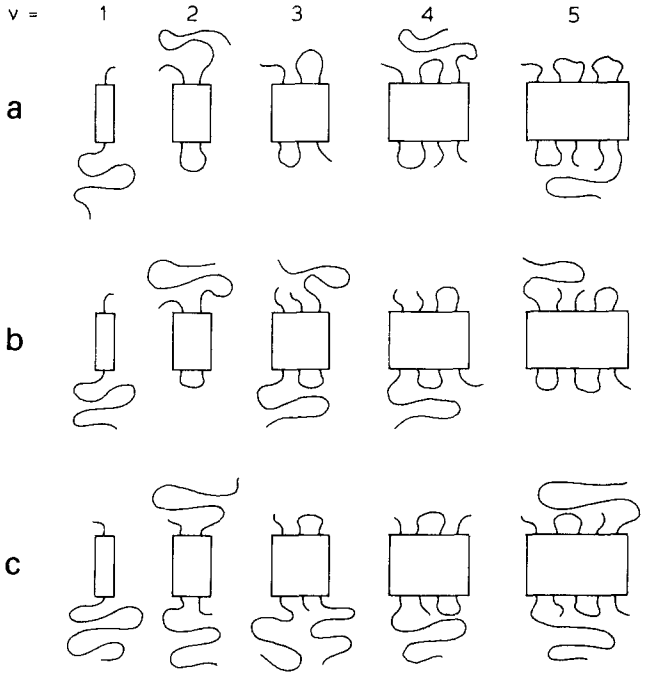

Figure 5 Three possible sequences for the growth of a surface nucleus with $n = 2$

(d) *Effect of l on σ_{e0} and σ_{ef}* In equations (9) we implied that σ_{e0} and σ_{ef} are independent of l and hence of the lengths of cilia and chain-folds that are formed during attachment of molecular stems. Furthermore, we shall employ values for these parameters measured on mature crystals (i.e. where cilia are short and chain-folds are tight). Sanchez and DiMarzio, however, pointed out that the presence of the crystal as an excluded volume reduces the number of conformations available to a cilium or a chain-fold, and indicated the effect this may have on the partition function[9]. The effect causes σ_{e0} and σ_{ef} to be l-dependent.

It is interesting to take the present theory to its limit of high *MW* and high degrees of folding, for comparison with results of previous authors. This may be done consistently by taking the limit as $\lambda \to \infty$ and allowing n to be a large but finite integer. From this it follows that $L \to \infty$,

$$\frac{j}{\eta_0} \simeq \frac{\alpha_0}{1+\gamma+\gamma^2+\ldots} = \alpha_0(1-\gamma) \tag{24}$$

and:

$$l_{min} \simeq \frac{2\sigma_{ef}}{\Delta f} \tag{25}$$

Expressing $\Sigma(j/\eta_0)$ in integral form we now obtain:

$$\sum\left(\frac{j}{\eta_0}\right) \simeq \frac{1}{l_u} \int_{2\sigma_{ef}/\Delta f}^{\infty} \alpha_0(1-\gamma)\mathrm{d}l \tag{26}$$

in agreement with Lauritzen and Hoffman[11]*. In evaluating α_0 a problem arises, as in the limit of high *MW* ($\lambda \to \infty$) the entropy of localization $k \ln Cp$ clearly does not apply. This implies a discontinuity between the low *MW* theory given here and the case of high *MW*, suggesting a gradual disappearance with increasing *MW* of the lengthwise molecular localization within the nucleus, which the present theory cannot describe in its basic form. Modifications (b) and (c) (Model 2), however, do not suffer from this difficulty. Incorporating this feature into α_0 and evaluating the integral in equation (26) we obtain:

$$\sum\left(\frac{j}{\eta_0}\right) \simeq \frac{\mu kT}{l_u} \exp\left(-\frac{2ab\sigma_{e0}}{kT} + \frac{2\psi ab\sigma_{ef}}{kT}\right) \exp\left(-\frac{4b\sigma\sigma_{ef}}{\Delta f kT}\right) \times \left\{\frac{1}{2b\sigma - \psi ab\Delta f} - \frac{1}{2b\sigma + (1-\psi)ab\Delta f}\right\} \tag{27}$$

* The approximate nature of equation (26) should be emphasized. It arises because it is not possible to take the limits $\lambda \to \infty$, $n \to \infty$, $L \to \infty$ simultaneously

which agrees with the corresponding expression of Lauritzen and Hoffman[11] when allowance is made for their approximation $\sigma_{e0} \simeq 0$.

Application to PEO

The theory given above was used to predict the crystal growth-rates, as functions of λ, n and T, for low *MW* PEO. Fortunately, detailed thermodynamic data are available for this polymer. We employ here the calorimetric results of Buckley and Kovacs[16,21] in preference to those of other workers[23–25] for reasons given before[21].

Let a superscript '0' denote equilibrium melting of a hypothetical large perfect crystal of infinite molecular weight polymer. Its melting point T_m^0 would be 68.9°C for PEO. For $T < T_m^0$ the bulk free enthalpy of fusion Δf can be approximated by:

$$\Delta f = \Delta h^0 \Delta T / T_m^0 \tag{28}$$

where $\Delta T = T_m^0 - T$ and Δh is the enthalpy of fusion: $\Delta h^0 = 2.42 \times 10^8$ J m^{-3} for PEO. Equation (28) neglects the specific heat difference between crystal and melt, but will be correct to within *c.* 1% over the temperature range of interest here.

The surface free energies σ_{e0} and σ_{ef} used here are strictly defined differently from those given before[16]. The latter contain the free enthalpy excess of cilia and chain-folds over that of an equivalent mass of crystal. Assuming the free enthalpy of surface layers approximates that of the melt, and denoting these previous values by $\tilde{\sigma}_{e0}$ and $\tilde{\sigma}_{ef}$ respectively, it is clear that:

$$\left.\begin{aligned} \sigma_{e0} &= \tilde{\sigma}_{e0} - l_{c0}\Delta f \\ \sigma_{ef} &= \tilde{\sigma}_{ef} - \tfrac{1}{2} l_{f0}\Delta f \end{aligned}\right\} \tag{29}$$

The distinction only arises of course at finite supercooling.

As pointed out before[21], the absolute magnitude of $\tilde{\sigma}_{e0}$ cannot be determined since it always appears in conjunction with the unknown constant C. Its value does, however, appear to increase from $n = 0$ to $n \geqslant 1$ because of hydrogen-bonding in the surfaces of extended-chain crystals; thus Buckley and Kovacs[16] found:

$$\left.\begin{aligned} \tilde{\sigma}_{e0}^0 + \frac{kT_m^0}{2ab} \ln C &= 2.31 \times 10^{-2} \text{ J m}^{-2} \quad (n = 0) \\ \tilde{\sigma}_{e0}^0 + \frac{kT_m^0}{2ab} \ln C &= 3.33 \times 10^{-2} \text{ J m}^{-2} \quad (n \geqslant 1) \\ \tilde{\sigma}_{ef}^0 &= 2.08 \times 10^{-2} \text{ J m}^{-2} \end{aligned}\right\} \tag{30}$$

These values were used in the present work, together with their estimated temperature coefficient[16] of -1.3%/deg C (compatible with the corresponding quantity for PE[26]). The chain-end surface free energy σ_{e0} enters the present theory only through σ'_{e0} (see equation (10)), which was therefore calculated from:

$$\sigma'_{e0} = \left(\tilde{\sigma}_{e0} + \frac{kT}{2ab} \ln C\right) - l_{c0}\Delta f + \frac{kT}{2ab} \ln p \tag{31}$$

The contour lengths of cilia and chain-folds were estimated[16] to be $l_{c0} = 9\, l_u$, $l_{f0} = 10\, l_u$ ($l_u = 0.0928$ nm). These must be considered approximate but their precise values are unimportant here. Even assuming extreme values of $l_{c0} = l_{f0} = 0$ produced closely similar results.

The crystal of PEO is monoclinic, and melt-grown crystals show chiefly {100} and {140} prism faces[3]. Parameters a and b were therefore taken equal to $|b|/2 = 0.652$ nm and $|a^*|/2 = 0.328$ nm respectively, appropriate to growth on {100} faces (see Takahashi and Tadokoro[27] for the crystallography of PEO).

It was not clear what value should be assigned to ψ (its apparently empirical nature is an unsatisfactory feature of the current theory). Inspection of equation (12), however, shows that $j/\eta_0 \to 0$ as $l \to \infty$ (as illustrated in *Figure 4*) only whilst:

$$\Delta T < 2\sigma T_m^0 / \psi a \Delta h^0 \tag{32}$$

At higher supercoolings j/η_0 diverges as $l \to \infty$ creating the 'δl catastrophy'[11]. Concurrently, there is a change in shape of the curves $G_1(T)$ and $G_2(T)$. Applying the inequality (32) to PEO gives the critical ΔT as 43 deg C when $\psi = 1$, yet experimental data in this region show no sign of a change in shape of the $G(T)$ relation[28]. Clearly, if the concept of ψ has physical meaning for PEO its value must be less than 1. In the present work a value of 0.5 was adopted, although checks made using $\psi = 0$ or $\psi = 1$ gave no significant difference in the curves $G_1(T)$ and $G_2(T)$ for the range of temperatures considered.

The remaining unknown is the lateral surface free energy σ. The true value for {010} faces of PEO is not known. Hoffman and co-workers[26] have suggested that in general it may be estimated from:

$$\sigma = x \Delta h (ab)^{1/2} \tag{33}$$

where x is a constant, approximately 0.1 for chain molecules. In the case of PEO this yields $\sigma = 0.0112$ J m^{-2}.

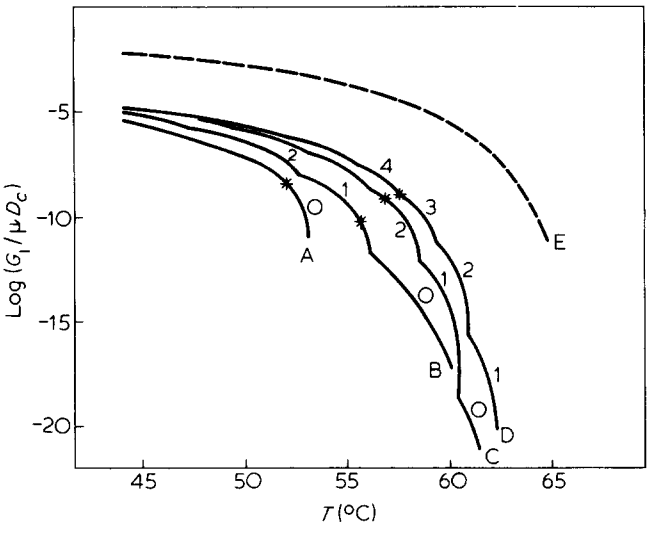

Figure 6 Crystal growth-rate G_1 *versus* temperature T predicted by equation (14) using equation (12) for the four low *MW* fractions of *Figure 1*, and using equation (27) for the limit of high *MW* when n is large. x is taken equal to 0.1 (σ = 0.0112 J m^{-2}). * indicates D_c^* = 1 μm

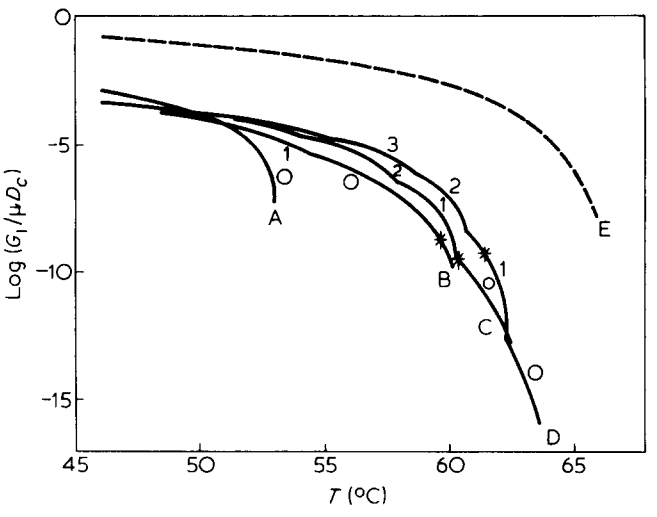

Figure 7 As for *Figure 6*, but with x = 0.05 (σ = 0.0056 J m^{-2})

The summations of equations (14) and (17) are conveniently carried out numerically. This is also the most realistic procedure physically if l is stepped by l_u, since each molecular stem must contain a whole number of main-chain atoms. This method was therefore adopted here. The summations were obtained over the range $L \geqslant l > l_{min}$, stepping l downwards from L in increments of l_u.

Figure 6 shows the curves of $G_1(T)$ which result for the four molecular weights referred to in *Figure 1*. Each curve has been calculated as a family of branches, each branch corresponding to a different value of n. We assume that growth occurs at any given temperature with the value of n which gives the highest growth-rate at that temperature. In addition, the high *MW* limit corresponding to equation (27) is shown, assuming in this case that $C = 1$. The predicted curves turned out to be highly sensitive to σ, whose precise value is uncertain. To illustrate this, *Figure 7* shows predictions obtained using x = 0.05 (σ = 0.0056 J m^{-2}).

G_2 and hence D_c^* were also calculated. D_c is not known. However, the fact that PEO crystal growth is found to be linear in time[4] to a resolution of the order of 1 μm indicates that in practice $D_c < 1$ μm. In *Figures 6* and *7* a star is used to indicate the point (temperature T^*) where the calculated $D_c^* = 1$ μm. At $T > T^*$, $D_c^* > 1$ μm; at $T < T^*$, $D_c < 1$ μm. Hence at $T > T^*$, régime 1 definitely obtains; whereas at $T < T^*$, the possibility of a transition to régime 2 cannot be ruled out.

DISCUSSION

The most striking feature of both *Figures 6* and *7* is their qualitative resemblance to the experimental data of Kovacs and co-workers given in *Figure 1*. The theory thus predicts chain-folding: a transition from extended-chain to folded-chain growth is predicted at sufficient supercooling, and folding is by adjacent re-entry.

It is interesting to examine why this occurs, in relation to the theory. For supercoolings of more than a few degrees, the expression for j/η_0 in equation (12) is dominated by the term $\exp(-2bl\sigma/kT)$. The maximum nucleation rate corresponds to l a little greater than l_{min} (*Figure 4*). *Figure 8* shows the variation of l with n and T predicted for *MW* = 5970: its minimum l_{min}, maximum L and mean $\langle l \rangle$, defined by:

$$\langle l \rangle = \frac{\Sigma[l_j(l)/\eta_0]}{\Sigma[j(l)/\eta_0]} \tag{34}$$

where the summations are from $l = l_{min}$ to $l = L$. It is now clear that the reason for increasing chain-folding with increasing supercooling is that at a given temperature l_{min} decreases with increasing n and hence $\exp(-2bl\sigma/kT)$ is increased. The reason for l_{min} decreasing with increasing n is the entropy of localization term $k \ln Cp$ which occurs in σ'_{e0} (equation (10)), and which has proportionately less effect on l_{min} as n increases (see equation (13)). (It is the same effect which causes extended-chain crystals of PEO to melt at a lower temperature than folded-chain crystals of equal thickness[16].

Some aspects of the calculations show quantitative agreement with experiment. Each branch of $G_1(T)$ and $G_2(T)$ is forced to approach zero at its corresponding melting-point measured by calorimetry, since the present theory is consistent with the analysis used previously for melting of PEO (substitute L for l_{min} in equation (13) and compare with equation (5) of reference 16) and we have chosen to use thermodynamic data measured in the previous study. In the case of $MW \to \infty$ and large n (equation (27)) the theory reduces to:

$$G_1 \propto \exp(-KT_m^0/T\Delta T) \tag{35}$$

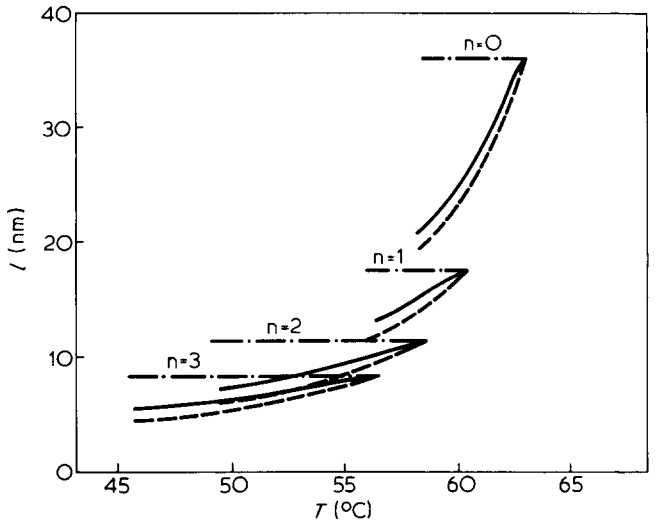

Figure 8 Three measures of predicted surface nucleus thickness l *versus* temperature T: L, $\langle l \rangle$ and l_{min} for a PEO fraction of MW = 5970. — · — · — · —, L; ——, $\langle l \rangle$; — — — — — —, l_{min}

where:

$$K = 4b\sigma\sigma_{ef}/k\Delta h^0 \tag{36}$$

at large supercooling. This equation is well-known to apply to a large number of high MW polymers[26], including PEO[3]. Even for finite MW, the present theory predicts that G_1 will converge to this relationship at sufficient supercooling ($l_{min} \ll L$) when n is large (see equation (12)), in agreement with experimental data for low MW PEO[3]. Applying equations (35) and (36) to their data for PEO, Kovacs and Gonthier[3]** obtained K = 127 deg C, whereas the thermodynamic data used here (with x = 0.1) yield K = 91 deg C (neglecting variation of σ_{ef} with T). Exact agreement with experiment could easily be obtained here by adjusting x to 0.14. It is interesting to note, however, that remarkably good agreement could also be obtained (K = 129 deg C) with x = 0.1, by choosing $b = \frac{1}{2}(|a^*|^2 + |b/2|^2)^{1/2} = 0.462$ nm, appropriate to {120} growth-faces. {120} faces are not observed in the optical microscope on melt-grown PEO crystals[3], although they do appear on solution-grown crystals[29]. This result therefore poses the question of whether melt-grown crystals do in fact have serrated edges, with {120} growth-faces, on a finer scale than can be resolved with the optical microscope (see Kovacs *et al.*[5]).

The present theory also sheds light on some qualitative features of the transitions in n. Firstly, the transitions as observed by Kovacs and co-workers[4] are very sharp, measurable to within 0.01°C, and the sharpness is greatest for transitions between low values of n. Theoretical curves such as those of *Figure 8* provide an explanation. Consider the transition n = 0 to n = 1 in *Figure 8*. In the region of this transition $l_{min}(n = 0) > L(n = 1)$. At temperatures below the transition, therefore, where once-folded-chain growth predominates, the substrate is too narrow to support any extended-chain nuclei† and mixing of n is prohibited. At temperatures above the transition, $G_1(T)$ for n = 1 decreases sharply as it approaches the corresponding melting point, also making mixing of n unlikely. For these reasons the transition will be sharp.

Secondly, it was noted by Kovacs and Gonthier[3] that at temperatures just above a transition, especially n = 0 to n = 1, crystals have no well-defined faces but appear rounded, implying very rough edges. This also can be explained from *Figure 8*. At temperatures just above the transition once-folded-chain nuclei can form on the extended-chain substrate, although they rapidly become rare as their melting-point is approached. When an occasional once-folded-chain layer does form, however, it can thicken immediately only to $L(n = 1)$ which (as mentioned above) is too small to support extended-chain nuclei. It therefore acts as a defect, locally blocking growth of the crystal. Events such as this, even though comparatively rare, would disrupt the perimeter of the crystal and could account for the rounded shapes observed.

Closer comparison of *Figures 1* and *6*, however, reveals quantitative discrepancies. The range of G_1 covered in the temperature range considered is far too large. In particular, the vertical separation between adjacent branches of the same curve is too large and the gradient of $G_1(T)$ is too great for low values of n. The predicted transition temperatures are too high, in some cases by several degrees.

Some contribution to these discrepancies certainly comes from two factors the theory cannot embrace. The curves in *Figures 6* and *7* represent $G_1/\mu D_c$. To obtain G_1/μ it is necessary to multiply by the morphological factor D_c. This is likely to be temperature and n-dependent, increasing within each branch as the crystal edges become less rough. This would have the effect of reducing the magnitude of the gradient of $G_1(T)$ within each branch. In addition, fractionation near the melting-points $T_m(n, p)$ will cause transition temperatures to be slightly lower than those predicted.

** Although Kovacs and Gonthier used T_m (n = 0, λ) in place of T_m^0 in applying equation (35), the effect of the discrepancy clearly disappears at large supercooling

† This is supported by the experimental fact that extended-chains cannot nucleate on a once-folded-chain substrate[4]

The major discrepancy, however, is in the vertical separation of adjacent branches of a given curve, which cannot be explained along these lines. The situation can be improved by assuming a smaller value for x (and hence σ) – see *Figure 7* – but this of course sacrifices the agreement with experiment at high supercooling using $x = 0.1$. Furthermore the discrepancy is in the wrong sense to be explicable in terms of a transition to régime 2 at high supercoolings.

The modifications (a) to (d) introduced above offer no help in this respect. (a) is not applicable as it merely justifies the formulation of G_1 used here. (b) and (d) were found to show only minor changes in the shape of the curves $G_1(T)$, insufficient to explain the discrepancy. Model 1 of (c) produced essentially step-like growth-rate branches, due to a rapid decrease of l_{min} to unreasonably low values (of the order of l_u) at the supercoolings considered, while model 2 did not even predict the transition from extended-chain to folded-chain growth.

The only remaining possibility, in terms of the present theory, is that σ increases with increasing n, converging on the case $x = 0.1$ at large n. However, there is no precedent for such behaviour and the explanation is unsatisfying. It is more likely that the discrepancy reflects a previously unsuspected weakness in the accepted kinetic model of polymer crystallization. This possibility merits further investigation, but is beyond the scope of the present paper.

During the course of this work, Point and Kovacs[30] have developed a new reduction rule for comparing polymer crystal growth-rate data with predictions of the kinetic theory. When applied to PEO, it too indicates a discrepancy between current theory and experimental results, in line with the present work[30].

CONCLUSIONS

We have shown that to extend the kinetic theory of polymer crystallization to finite molecular weights requires considerably more detailed knowledge of the growth process than is sufficient for the high *MW* limit. Only in the case of PEO is existing knowledge sufficient for a suitable theory to be constructed with any confidence. Even then several points of ambiguity remain, which have been explored here by considering modifications to the theory.

The main conclusion of the present work is that when the kinetic theory, suitably modified for low *MW* PEO, is compared with detailed growth-rate data for this system, extensive qualitative agreement is obtained. In particular, the theory predicts increasing chain-folding with increasing supercooling or *MW*. It emerges as a consequence of assuming that when molecules attach to a growth nucleus they have no freedom of lengthwise positioning within it. This may apply to other polymers and hence be a general explanation for chain-folding. If the entropies of cilia and chain-folds are taken into account, one would expect molecules first to attach near one of their ends[1,19] and then to form tight folds[9] (see also the Appendix). This situation gives the lowest surface free energy, but also requires the molecules to have no choice of lengthwise positioning in the nucleus. Until similar results are obtained for other polymer systems, however, we cannot be certain that the effect is not special to PEO, perhaps being associated with hydroxyl end-group pairing.

Minor points are that the theory can also rationalize the sharpness of the transitions in growth-rate curves, and the changes in crystal shape near the transitions. When taken to its limit of high *MW* and large n, the theory converges on the existing theory of Lauritzen and Hoffman[10]. In this case, reasonable quantitative agreement with experiment is obtained, suggesting either that σ is slightly larger than previously suspected or that crystals are serrated, with small-scale growth-faces of type {120}

Detailed comparison between theory and experiment, however, reveals a sizable discrepancy in the relative levels of growth-rate in adjacent branches of the same curve. This can be empirically explained by allowing σ to increase with increasing chain-folding, but alternatively a new weakness in the kinetic model of polymer crystallization may have been revealed. It seems that the discrepancy cannot be removed within the framework of existing theory.

APPENDIX

(a) Choice of sequence

Consider the nucleation rate given by equation (3):

$$\frac{j}{\eta_0} = \frac{\alpha_0}{[1 + \gamma_1 + \gamma_1\gamma_2 + \gamma_1\gamma_2\gamma_3 + \dots]} \tag{A1}$$

We indicated before that it is reasonable to assume there to be only two distinct γ_v: γ and γ'. For low *MW* PEO, provided *MW* is not too low, we have $\sigma'_{e0} > \sigma_{ef}$, and hence from equation (11) $\alpha < \alpha'$ and $\gamma < \gamma'$. In equation (A1), therefore, the upper limit on nucleation rate results when all occurrences of γ appear as early as possible in the infinite series, giving for the case $n = 2$:

$$\frac{j}{\eta_0} = \frac{\alpha_0}{[1 + \gamma + \gamma^2 + \gamma^2\gamma' + \gamma^3\gamma' + \dots]}; \tag{A2}$$

whereas the lower limit results when occurrences of γ' appear as early as possible, giving for $n = 2$:

$$\frac{j}{\eta_0} = \frac{\alpha_0}{[1 + \gamma' + \gamma'\gamma + \gamma'\gamma^2 + (\gamma')^2\gamma^2 + \dots]} \tag{A3}$$

Inspection shows that in both upper and lower limits the sequence must continue by each molecule folding fully n times before addition of the next. Equation (A2) corresponds to the sequence beginning as in *Figure 5a*, and equation (A3) as in *Figure 5c*. It is now clear that G_1 and G_2 calculated before apply to the sequence giving the highest nucleation rate. This is our justification for assuming that particular sequence. Modified forms for equation (8) and hence G_1 and G_2 are easily derived from equation (3), for the lower limit on j/η_0 (g is unchanged because the repeating sequences of α_v and γ_v are unchanged).

(b) Number of nucleation sites

There are $l/3l_u$ monomer units in one molecular stem of the nucleus and $L/3l_u$ in the crystal substrate. If the only requirement is that monomer units in nucleus and substrate are in register, there are $\tilde{\omega}$ possible lengthwise positions of the nucleus, where $\tilde{\omega}$ is the nearest integer below ω, given by:

$$\omega = (L - l + 1)/3l_u \tag{A4}$$

Incorporating this into the theory simply involves multiplying α_0 by $\tilde{\omega}$.

(c) Degree of molecular localization

Model 1 Suppose that the $l/3l_u$ monomer units of each stem can be chosen randomly from the $L/3l_u$ units of the molecule it will comprise after thickening. This appears to correspond to the model of Beech *et al.*[8]. In this case the first stem of the first molecule can be selected in $(n + 1)\tilde{\omega}$ different ways, first stems of subsequent molecules in $\tilde{\omega}$ ($n = 0$) or $2\tilde{\omega}$ ($n > 0$), and subsequent stems of first and subsequent molecules in $\tilde{\omega}$ ways. The theory is therefore simply modified by multiplying α_0 by $(n + 1)\tilde{\omega}$, α' by $\tilde{\omega}$ ($n = 0$) or $2\tilde{\omega}$ ($n > 0$), and α by $\tilde{\omega}$.

Model 2 Suppose that the length of all folds as-formed is always l_{f0}, (for justification see Sanchez and DiMarzio[9]). Then at the ith stage of the addition of a molecule there is a string of p_i consecutive monomer units, where:

$$p_i = (il + 2l_{c0} + (i - 1)l_{f0})/3l_u \tag{A5}$$

to be chosen from the p units of the molecule. If this choice is made randomly, the nucleus will have an additional entropy:

$$k \ln (p - p_i + 1)$$

associated with this freedom. Assuming that this appears in forward transition rates only, it is possible to construct the terms required in G_1 as follows:

$$\left.\begin{aligned}
\alpha_0 &= \mu \exp\left[-\frac{2bl\sigma}{kT} - \frac{2ab\sigma'_{e0}}{kT} + \ln(p - p_1 + 1) + \frac{\psi abl\Delta f}{kT}\right] \\
\alpha_i &= \mu \exp\left[-\frac{2ab\sigma_{ef}}{kT} + \ln\left\{\frac{p - p_{(i+1)} + 1}{p - p_i + 1}\right\} + \frac{\psi abl\Delta f}{kT}\right] \qquad (i = 1, 2, \ldots n) \\
\alpha_{n+1} &= \mu \exp\left[-\frac{2ab\sigma'_{e0}}{kT} + \ln(p - p_1 + 1) + \frac{\psi abl\Delta f}{kT}\right]
\end{aligned}\right\} \tag{A6}$$

with β_v remaining unchanged. Although the periodicity of α_v (and hence γ_v) is preserved, we now find that α_v depends on v within $1 \leqslant v \leqslant n$, and so equations (8) and (20) do not apply. It is necessary to revert to equation (5) for j/η_0 and equation (19) for g. In this way G_1 and G_2 may be determined.

(d) Effect of l on σ_{e0} and σ_{ef}

According to Sanchez and DiMarzio[9], the free enthalpies of cilia containing Cp_c 'statistical segments' and chain-folds containing Cp_f will be increased by:

$$\left.\begin{aligned}
\Delta\phi_c &= kTk_c \ln Cp_c \\
\Delta\phi_f &= kTk_f \ln Cp_f
\end{aligned}\right\} \tag{A7}$$

respectively, by the excluded volume of the crystal reducing the number of conformations available to them (p_c and p_f are the respective numbers of monomer units involved). Constants k_c and k_f can be estimated to be 0.5 and 1 respectively[9]. We therefore need to estimate each p_f and p_c arising. To give this problem a unique solution we introduce another variant on our model of the growth process. Suppose p_{c0}, p_{f0} correspond to the situation in a mature crystal (thickness L) and are the minimum possible values of p_c, p_f. If we adopt the criterion of always minimizing the contributions of $\Delta\phi_c$ and $\Delta\phi_f$, then we reach the conclusion that at any stage in the deposition of a molecule one cilium will be of minimum length p_{c0}, all m folds

will be of minimum length p_{f0}, and so the other cilium will be of length $p - p_n - p_{c0} - mp_{f0}$ where p_n is the number of monomer units $(m + 1)l/3l_u$ which have so far crystallized. This model corresponds to that envisaged by Hoffman *et al.*[1]. Under these circumstances, $\Delta\phi_c$ and $\Delta\phi_f$ for the first cilium and all folds apply to p_{c0} and p_{f0} respectively, and are therefore included in the measured σ_{e0} and σ_{ef} from mature crystals. The necessary modification to the theory therefore is that the free enthalpy at each stage in the growth sequence is greater by an amount:

$$kTk_c \ln [(p - p_n - p_{c0} - mp_{f0})/p_{c0}]$$

than was allowed for previously, due to the additional length of the long cilium. Replacing in this expression numbers of monomer units by their physical lengths, i.e. p by λ, p_n by $(m + 1)l$, p_{c0} by l_{c0}, and p_{f0} by l_{f0}, we find that the transition rates become:

$$\alpha_0 = \mu \exp \left[-\frac{2bl\sigma}{kT} - \frac{2ab\sigma'_{e0}}{kT} - k_c \ln [(\lambda - l - l_{c0})/l_{c0}] + \frac{\psi abl\Delta f}{kT} \right]$$

$$\alpha_\upsilon = \mu \exp \left[-\frac{2ab\sigma_{ef}}{kT} - k_c \ln \{[\lambda - (\upsilon + 1)l - l_{c0} - \upsilon l_{f0}]/[\lambda - \upsilon l - l_{c0} - (\upsilon - 1)l_{f0}]\} + \frac{\psi abl\Delta f}{kT} \right] \quad (\upsilon = 1, 2, \ldots n) \text{ (A8)}$$

$$\alpha_{n+1} = \mu \exp \left[-\frac{2ab\sigma'_{e0}}{kT} - k_c \ln [(\lambda - l - l_{c0})/l_{c0}] + \frac{\psi abl\Delta f}{kT} \right]$$

As in the previous case, it is necessary to revert to equation (5) for j/η_0 and equation (19) for g in order to evaluate G_1 and G_2.

ACKNOWLEDGEMENTS

The author is grateful to Drs A. J. Kovacs and J. J. Labaig for a stimulating correspondence on the subject treated in this paper.

REFERENCES

1 Hoffman, J. D., Frolen, L. J., Ross, G. S. and Lauritzen, J. I. *J. Res. N.B.S.* 1975, **79A**, 671
2 Labaig, J. J., *Thesis*, Univ. L. Pasteur, Strasbourg, 1978
3 Kovacs, A. J. and Gonthier, A. *Kolloid-Z.u.Z. Polym.* 1972, **250**, 530
4 Kovacs, A. J., Gonthier, A. and Straupe, C. *J. Polym. Sci. (C)* 1975, **50**, 283
5 Kovacs, A. J., Straupe, C., and Gonthier, A. *J. Polym. Sci. (C)* 1977, **59**, 31
6 Kovacs, A. J. and Straupe, C. *J. Crystal Growth* to be published
7 Mandelkern, L., Fatou, J. G. and Howard, C. *J. Phys. Chem.* 1965, **69**, 956
8 Beech, D. R., Booth, C., Hillier, I. H. and Pickles, C. J. *Eur. Polym. J.* 1972, 8, 799
9 Sanchez, I. C. and DiMarzio, E. A. *J. Chem. Phys.* 1971, **55**, 893
10 Lauritzen, J. I. and Hoffman, J. D. *J. Res. N.B.S.* 1960, **64A**, 73
11 Lauritzen, J. I. and Hoffman, J. D. *J. Appl. Phys.* 1973, **44**, 4340
12 Lauritzen, J. I. *J. Appl. Phys.* 1973, **44**, 4353
13 Arlie, J. P., Spegt, P. A. and Skoulios, A. E. *Makromol. Chem.* 1966, **99**, 160
14 Arlie, J. P., Spegt, P. A. and Skoulios, A. E. *Makromol. Chem.* 1967, **104**, 212
15 Spegt, P. A. *Makromol. Chem.* 1970, **140**, 167
16 Buckley, C. P. and Kovacs, A. J. *Colloid Polym. Sci.* 1976, **254**, 695
17 Spegt, P. A. *Makromol. Chem.* 1970, **139**, 139
18 Frank, F. C. and Tosi, M. *Proc. R. Soc. (A)* 1961, **263**, 323
19 DiMarzio, E. A. *J. Chem. Phys.* 1967, **47**, 3451
20 Flory, P. J. and Vrij, A. *J. Am. Chem. Soc.* 1963, **85**, 3548
21 Buckley, C. P. and Kovacs, A. J. *Progr. Colloid Polym. Sci.* 1975, **58**, 44
22 Sanchez, I. C. and DiMarzio, E. A. *J. Res. N.B.S.* 1972, **76A**, 213
23 Ashman, P. C. and Booth, C. *Polymer* 1972, **13**, 459
24 Beech, D. R., Booth, C., Pickles, C. J., Sharpe, R. R. and Waring, J. R. S. *Polymer* 1972, **13**, 246
25 Afifi-Effat, A. M. and Hay, J. N. *J. C. S. Faraday II*, 1972, **68**, 656
26 Hoffman, J. D., Davis, G. T. and Lauritzen, J. I. in 'Treatise on Solid State Chemistry' (N. B. Hannay, ed.) Vol. 3, Plenum Press, New York, 1976, Ch 6
27 Takahashi, Y. and Tadokoro, H. *Macromolecules* 1973, **6**, 672
28 Kovacs, A. J. Private communication
29 Lotz, B. and Kovacs, A. J. *Kolloid-Z.u.Z. Polym.* 1966, **209** 97
30 Point, J. J. and Kovacs, A. J. *Macromolecules* to be published